



Year: 2020

Load-bearing capacity of CAD/CAM 3D-printed zirconia, CAD/CAM milled zirconia, and heat-pressed lithium disilicate ultra-thin occlusal veneers on molars

Ioannidis, A ; Bomze, D ; Hämmerle, C H F ; Hüsler, J ; Birrer, O ; Mühlemann, S

Abstract: **OBJECTIVES:** The load-bearing capacity of ultra-thin occlusal veneers made of 3D-printed zirconia were compared to the ones obtained by fabricating these reconstructions by CAD/CAM milling zirconia or heat-pressing lithium-disilicate. **METHODS:** On 60 extracted human molars, the occlusal enamel was removed and extended into dentin. Occlusal veneers of 0.5 mm thickness were digitally designed. The specimens were divided into 3 groups (n = 20 each) differing in the restorative material and the fabrication technique of the occlusal veneer. (1) 3DP: 3D-printed zirconia (Lithoz); (2): CAM: milled zirconia (Ceramill Zolid FX); (3) HPR: heat-pressed lithium disilicate (IPS e.max Press). After conditioning procedures, the restorations were adhesively bonded onto the conditioned tooth. Thereafter, all specimens were aged in a chewing simulator by exposure to cyclic fatigue and temperature variations. Subsequently the specimens were statically loaded and the load which was necessary to decrease the maximum load by 20% and initiate a crack ($F_{initial}$) and the load which was needed to fracture the specimen (F_{max}) were measured. Differences between the groups were compared applying the Kruskal-Wallis (KW) test and the Wilcoxon-Mann-Whitney-Test (WMW: $p < 0.05$). **RESULTS:** The median $F_{initial}$ values for the groups 3DP, CAM and HPR were 1'650 N, 1'250 N and 500 N. The differences between all three groups were statistically significant (KW: $p < 0.0001$). The median F_{max} values amounted to 2'026 N for the group 3DP, 1'500 N for the group CAM and 1'555 N for the group HPR. Significant differences were found between 3DP and CAM (WMW: $p = 0.0238$). **SIGNIFICANCE:** Regarding their load-bearing capacity, 3D-printed or milled zirconia, as well as heat-pressed lithium disilicate, can be recommended as restorative material for ultra-thin occlusal veneers to prosthetically compensate for occlusal tooth wear. Despite statistically significant differences between the restoration materials, all load-bearing capacities exceeded the clinically expected normal bite forces.

DOI: <https://doi.org/10.1016/j.dental.2020.01.016>

Posted at the Zurich Open Repository and Archive, University of Zurich

ZORA URL: <https://doi.org/10.5167/uzh-187750>

Journal Article

Accepted Version



The following work is licensed under a Creative Commons: Attribution-NonCommercial-NoDerivatives 4.0 International (CC BY-NC-ND 4.0) License.

Originally published at:

Ioannidis, A; Bomze, D; Hämmerle, C H F; Hüsler, J; Birrer, O; Mühlemann, S (2020). Load-bearing capacity of CAD/CAM 3D-printed zirconia, CAD/CAM milled zirconia, and heat-pressed lithium disilicate ultra-thin occlusal veneers on molars. *Dental Materials*, 36(4):e109-e116.
DOI: <https://doi.org/10.1016/j.dental.2020.01.016>



ELSEVIER

Available online at www.sciencedirect.com

ScienceDirect

journal homepage: www.intl.elsevierhealth.com/journals/dema

Load-bearing capacity of CAD/CAM 3D-printed zirconia, CAD/CAM milled zirconia, and heat-pressed lithium disilicate ultra-thin occlusal veneers on molars

A. Ioannidis^{a,*}, D. Bomze^b, C.H.F. Hämmerle^a,
J. Hüsler^c, O. Birrer^d, S. Mühlemann^a

^a Clinic of Reconstructive Dentistry, Center of Dental Medicine, Switzerland

^b Lithoz GmbH, Vienna, Austria

^c Department of Mathematical Statistics, University of Bern, Switzerland

^d Master Student, Center of Dental Medicine, University of Zurich, Switzerland

ARTICLE INFO

Article history:

Accepted 14 January 2020

Available online xxx

Keywords:

Ceramics

3D printing

Zirconia

Dental porcelain

Lithium-disilicate ceramic

Computer-aided design

Computer-aided manufacturing

Occlusal dental veneers

Fatigue

ABSTRACT

Objectives. The load-bearing capacity of ultra-thin occlusal veneers made of 3D-printed zirconia were compared to the ones obtained by fabricating these reconstructions by CAD/CAM milling zirconia or heat-pressing lithium-disilicate.

Methods. On 60 extracted human molars, the occlusal enamel was removed and extended into dentin. Occlusal veneers of 0.5 mm thickness were digitally designed. The specimens were divided into 3 groups (n = 20 each) differing in the restorative material and the fabrication technique of the occlusal veneer. (1) 3DP: 3D-printed zirconia (Lithoz); (2) CAM: milled zirconia (Ceramill Zolid FX); (3) HPR: heat-pressed lithium disilicate (IPS e.max Press). After conditioning procedures, the restorations were adhesively bonded onto the conditioned tooth. Thereafter, all specimens were aged in a chewing simulator by exposure to cyclic fatigue and temperature variations. Subsequently the specimens were statically loaded and the load which was necessary to decrease the maximum load by 20% and initiate a crack (F_{initial}) and the load which was needed to fracture the specimen (F_{max}) were measured. Differences between the groups were compared applying the Kruskal-Wallis (KW) test and the Wilcoxon-Mann-Whitney-Test (WMW: $p < 0.05$).

Results. The median F_{initial} values for the groups 3DP, CAM and HPR were 1'650 N, 1'250 N and 500 N. The differences between all three groups were statistically significant (KW: $p < 0.0001$). The median F_{max} values amounted to 2'026 N for the group 3DP, 1'500 N for the group CAM and 1'555 N for the group HPR. Significant differences were found between 3DP and CAM (WMW: $p = 0.0238$).

* Corresponding author at: Clinic of Reconstructive Dentistry, Center of Dental Medicine, University of Zurich Plattenstrasse 11, CH-8032, Zurich, Switzerland.

E-mail address: alexis.ioannidis@zzm.uzh.ch (A. Ioannidis).

<https://doi.org/10.1016/j.dental.2020.01.016>

0109-5641/© 2020 The Academy of Dental Materials. Published by Elsevier Inc. All rights reserved.

Significance. Regarding their load-bearing capacity, 3D-printed or milled zirconia as well as heat-pressed lithium disilicate can be recommended as restorative material for ultra-thin occlusal veneers to prosthetically compensate for occlusal tooth wear. Despite statistically significant differences between the restoration materials, all load-bearing capacities exceeded the clinically expected normal bite forces.

© 2020 The Academy of Dental Materials. Published by Elsevier Inc. All rights reserved.

1. Introduction

Extensive tooth wear and/or erosive substances can result in loss of occlusal tooth substance. A prosthetic rehabilitation may be necessary to compensate the lost tooth substance and to eliminate the associated symptoms. Traditional treatment concepts propose to restore the worn dentition by means of full-crown restorations [1]. However, these concepts involve a further loss of healthy tooth substance by extensive preparation of the already impeded dentition [2]. Nowadays, ultra-thin occlusal veneers represent an appropriate treatment alternative in cases of extensive erosive or abrasive tooth substance loss [3]. Zirconia and lithium disilicate ceramic are both eligible materials for these kind of minimally invasive restorations [4–6].

With the introduction of computer-aided design/computer-aided manufacturing (CAD/CAM), the processing of the high-strength ceramic zirconia has become possible [7–9]. Zirconia reconstructions are usually milled out of pre-fabricated zirconia blanks by subtractive manufacturing. The milling process is commonly performed using a pre-sintered condition of the zirconia blank. In this state, zirconia has a low inherent strength and the fabrication of ultra-thin reconstructions can be challenging [6]. More lately, additive manufacturing techniques have been introduced to fabricate high strength ceramics by lithography-based ceramic manufacturing (LCM) [10]. This technique allows to fabricate complex three-dimensional structures with high accuracy [10]. By 3D printing zirconia, restorations in a high resolution and thin walls can be produced [11]. The fabrication of heat-pressed lithium disilicate reconstructions exhibiting thin wall thicknesses is a regular procedure and showed a good reliability [6,12].

Both materials, zirconia and lithium disilicate, demonstrate an improved fracture toughness and higher flexural strength in comparison to conventional glass ceramics [13,14]. A study compared the mechanical performance of occlusal veneers made out of either zirconia or lithium disilicate [15]. It was found that being bonded to dentin, the load-bearing capacity of lithium disilicate is about 57% of the load-bearing capacity of zirconia [15]. Accordingly, another study revealed a median load-bearing capacity of 2'493 N for zirconia and 1'165 N for lithium disilicate restorations in 0.5 mm thickness when bonded to dentin [16]. The results of both groups surpassed the suggested fracture toughness for posterior reconstructions by far [17]. Thus, both materials are mechanically appropriate for the use as ultra-thin occlusal veneers in the posterior region.

Up to now, there is no study available in the literature, comparing the mechanical performance of 3D-printed occlusal

veneers made of zirconia to more traditionally applied fabrication techniques using conventional ceramic materials. Therefore, the objective of this study was to test whether the load-bearing capacity of ultra-thin 3D-printed zirconia occlusal veneers on molars exhibit differing load-bearing capacities if compared to CAD/CAM milled zirconia or pressed lithium-disilicate ceramic reconstructions.

2. Material and methods

2.1. Groups

The groups differed in the used restorative material (Table 1) and the fabrication technique. In total, 3 groups of 20 specimens each ($n = 20$) were included: (1) “3DP”: 3D-printed occlusal veneers made out of zirconia (Lithoz, Vienna, Austria); (2) “CAM”: CAD/CAM-fabricated occlusal veneers milled out of zirconia (Ceramill Zolid FX; Amann Girrbach, Pforzheim, Germany); (3) “HPR”: heat-pressed occlusal veneers made out of lithium-disilicate ceramic (IPS e.max press; Ivoclar Vivadent, Schaan, Liechtenstein).

2.2. Specimen preparation

In total, 60 extracted and intact human molars were inserted in an acrylic hollow cylinder made out of acrylic glass. The apical part of the tooth was embedded in self-curing resin (Technovit 4071; Kulzer, Wasserburg, Germany). To create typical defects for attrition or erosion, the occlusal enamel of the crown was removed until exposure of the dentin. Furthermore, fissures were slightly opened and sharp edges were rounded off. The specimens were randomly allocated to one of the study groups. During the complete study, the specimens were stored in distilled water.

2.3. Scanning procedures and restoration design

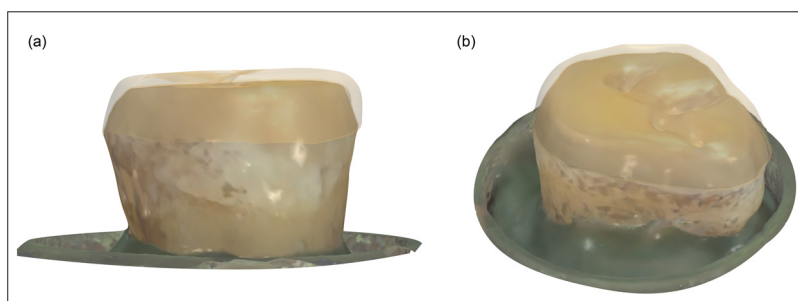
An optical impression of the prepared tooth was taken by means of a desktop scanner (Identica 3D Scanner; Dental Concept Systems, Ulm, Germany) and transmitted to a design software (3Shape software; Copenhagen, Denmark). Occlusal veneers were designed with a homogenous thickness of 0.5 mm (Fig. 1).

2.4. Fabrication of the restorations

According to the group allocation, the ceramic restorations were fabricated.

Table 1 – Restorative materials and respective compositions for the groups 3DP, CAM and HPR.

Group	Restorative material	Chemical composition
3DP	Zirconia (Lithoz, Wien, Austria)	ZrO ₂ + HfO ₂ + Y ₂ O ₃ + Al ₂ O ₃ (99.95 wt%), Y ₂ O ₃ (5,4–5,8 wt%), Al ₂ O ₃ (0.15–0.35 wt%),
CAM	Zirconia (Ceramill zolid FX, Amann Girrba ch, Pforzheim Germany)	ZrO ₂ (90.4–94.5 wt%), Y ₂ O ₃ (4–6 wt%), HfO ₂ (1.5–2.5 wt%), Al ₂ O ₃ (0–0.3 wt%), Er ₂ O ₃ (0–0.5 wt%), Fe ₂ O ₃ (0–0.3 wt%)
HPR	Lithium disilicate ceramic (IPS e.max Press; Ivoclar Vivadent, Schaan, Liechtenstein)	SiO ₂ (57–80 wt%), Li ₂ O (11–19 wt%), K ₂ O (0–13 wt%), P ₂ O ₅ (0–11 wt%), ZrO ₂ (0–8 wt%), ZnO (0–8 wt%), other oxides and ceramic pigments (0–10 wt%)

**Fig. 1 – Specimen and digitally designed semi-transparent depicted restoration from (a) lateral and (b) latero-occlusal.**

2.4.1. Group 3DP: fabrication procedures

The occlusal veneers of the group 3DP were fabricated by means of the Lithography-based Ceramic Manufacturing (LCM) process, which is based on the concept of photopolymerization (Fig. 2) [18,19]. Ceramic powder was dispersed into a mixture of photo-curable monomers to create the ceramic slurry (LithaCon 3Y 610 white; Lithoz, Vienna). The materials processed by LCM-technology were slurries comprising a photopolymerizable monomer mixture (dynamic viscosity at 20 °C is 43 Pa s) filled with various types of ceramic powder (3 mol% Y₂O₃ stabilized ZrO₂ in a purity of 99.9%) in a concentration of 40–60 Vol%. A thin layer of this slurry was automatically coated onto the vat, which is an assembly with transparent glass bottom. Thereafter, the building platform approached the vat, only leaving a small gap of 25 μm, which was filled with slurry. This gap correlates to the thickness of an individual layer in the green part. Consecutively, the photosensitive compounds comprised within this slurry were cured by selective exposure with blue light (wavelength 460 nm). Where this light hit the ceramic-filled slurry, the monomers photopolymerized into a 3-dimensional network, which then acted as a cage for the ceramic filler. After completing the layer, the building platform was elevated and the whole sequence was repeated all over again. The occlusal veneers were layered perpendicular to the tooth axis. The scaling factor was in XY-direction 1.358× and in Z-direction 1.370× to compensate for the sinter-shrinkage. After the layer-by-layer structuring using the CeraFab 7500-system (Lithoz, Vienna) the green parts were cleaned from the excess slurry by using compressed air and an appropriate solvent (LithaSol 20, Lithoz) capable of dissolving the slurry without damaging the cured structure. Postprocessing involved the debinding of the green part in which the organic photopolymer matrix was removed through pyrolysis at step-wise raising temperatures between 115 and 1'450 °C. Then, the resulting white parts were sintered in a high-temperature

(1'450 °C, 2 h) furnace (Nabertherm HTCT 08/16; Nabertherm, Lilienthal, Germany) to fully density (99.3%). Thereafter, the supporting structure was cautiously removed (Fig. 3).

2.4.2. Group CAM: fabrication procedures

The ceramic restorations of the group CAD were directly milled out of pre-fabricated zirconia discs (Ceramill Zolid FX; Amann Girrba ch) using a 5-axis milling machine (Ceramill Motion2 5×; Amann Girrba ch). Thereafter, the restorations were sintered to full density according to the manufacturer's instructions (Ceramill Therm S; Amann Girrba ch).

2.4.3. Group HPR: fabrication procedures

For the ceramic restorations of the group HPR, first, a PMMA template was milled out of a pre-fabricated ingot (Ceramill PMMA; Amann Girrba ch) by means of a 5-axis milling machine (Ceramill Motion2 5×; Amann Girrba ch). The templates were then used to produce pressed lithium disilicate restorations applying the “lost-wax and press-technique” and following the manufacturer's instructions. For this purpose, the PMMA-templates were fixed by a wax sprue (IPS Multi Wax Pattern Form A; Ivoclar Vivadent) and vested (IPS PressVEST Premium; Ivoclar Vivadent) into a mold. In an oven (KaVo EWL 5645; KaVo, Kloten, Switzerland), the vested templated was heated to complete dissolution: rate of 5 °C min⁻¹ from room temperature to 850 °C (holding time 60 min). Thereafter, into the resulting void, lithium-disilicate ceramic (IPS e.max Press; Ivoclar Vivadent) was heat-pressed in a heat-pressing sintering-oven (Programat EP 5010; Ivoclar Vivadent): rate 60 °C min⁻¹ from 700 °C to 898 °C (holding time 25 min). After cooling, the restorations were carefully devested and cleaned from the investing material by air-abrasion (50 μm Al₂O₃; Cobra, Renfert GmbH, Hilzingen, Germany) at a pressure of 2 bar. The surface was glazed and again placed into the sintering-oven.

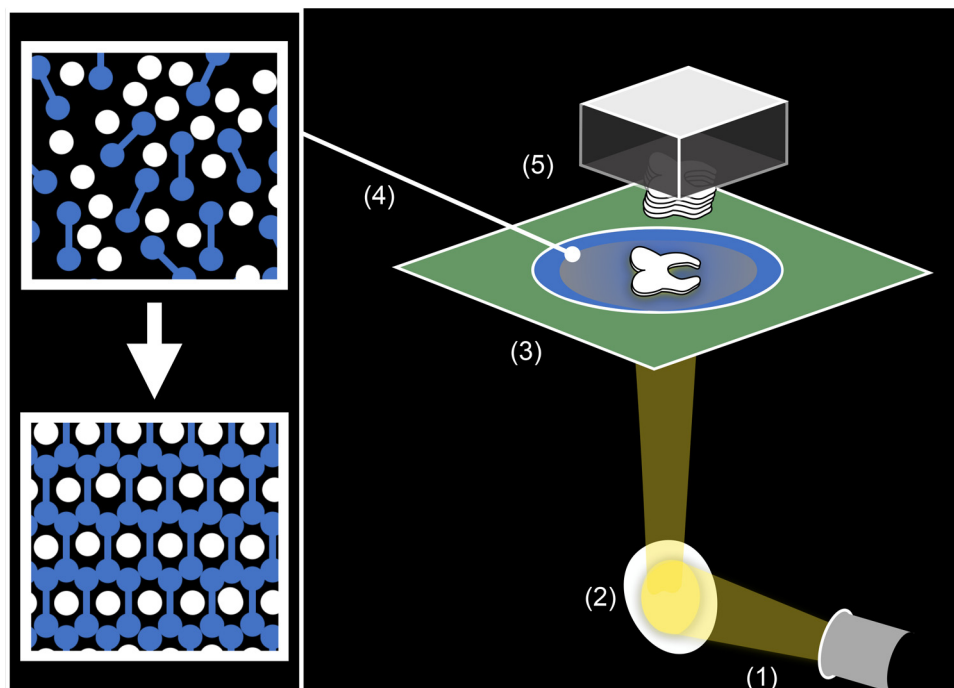


Fig. 2 – Schematic drawing of the 3D printer, producing the occlusal veneers of group 3DP with the Lithography-based Manufacturing process. In this process, LED light of 460 nm wavelength (1) hits a digital micro mirror device (2). In this device, micro mirrors can be positioned in an activated or in a deactivated position. By activating or deactivating the mirrors, light can be selectively transmitted to the vat (3). The vat itself is filled with a slurry of ceramic powder (white symbols) dispersed in a mixture of photo-curable monomers (blue symbols) (4). Where the light hits the ceramic-filled slurry, the monomers photo-polymerize into a 3-dimensional network, which then acts as a cage for the ceramic filler. The building-platform takes up the 3-dimensional network layer by layer (For interpretation of the references to color in this figure legend, the reader is referred to the web version of this article.).

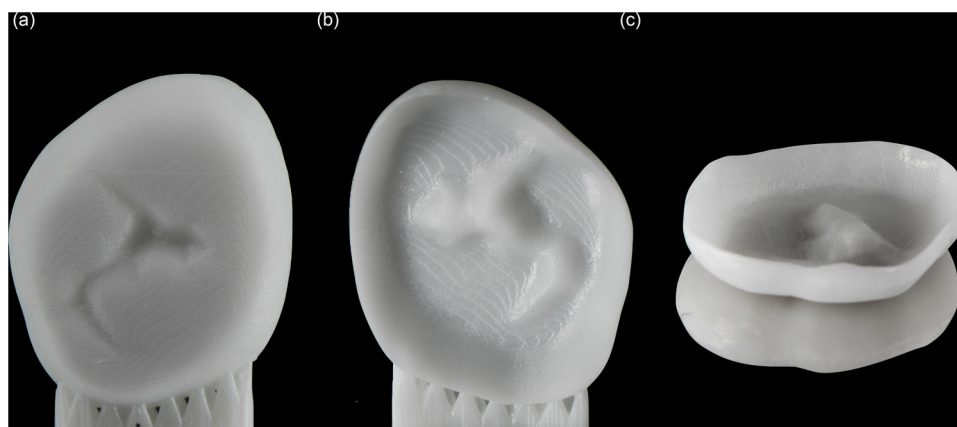


Fig. 3 – 3D-printed occlusal veneer before removing the support structures resulting from the printing process with (a) view from occlusal and (b) view on the inner surface. 3D-printed occlusal veneer (c) after having removed the supporting structure.

2.5. Cementation protocols

The conditioning procedure of the inner surface of the ceramic restoration varied according to the groups. In group HPR, etching for 20 s with 5% hydrofluoric acid (IPS ceramic etching gel; Ivoclar Vivadent) followed by water-spraying and air-drying. In groups 3DP and CAM, air-abrasion was applied to the inner

parts (Rocatec Plus 30 μm , 2.5 bar; 3 M ESPE, Seefeld, Germany). In all groups, a silane (Monobond Plus; Ivoclar Vivadent) was used and gently air-dried after 60 s. The enamel and the dentin of all specimens were etched with 35% phosphoric acid for 30 s (Ultraetch; Ultradent, Utah, USA). The surface was thereafter water-sprayed (30 s) and air-dried. An adhesive (Syntac Primer/Syntac Adhesive; Ivoclar Vivadent) was used for the

dentinal parts. A bonding agent (Heliobond; Ivoclar Vivadent) was applied to the tooth surface and to the ceramic restorations and after 20 s gently air-blown. The restorations were adhesively cemented using a dual-curing resin cement (Variolink Esthetic DC; Ivoclar Vivadent). After removal of excess cement, light-curing was performed (6×40 s).

2.6. Aging procedures

A chewing simulator [20] was used to age the specimens by a vertical indenter (rounded tip of \emptyset 8 mm) executing a vertical movement of 1 mm in a perpendicular direction to the occlusal plane ($1'200'000$ cycles of 49 N force at 1.67 Hz loading frequency) and thermo-cycling ($5-55$ °C and a dwelling time of 120 s). After aging, the specimens were evaluated under a stereomicroscope (magnification $1.25\times$) to check for integrity.

2.7. Static loading

The aged specimens were loaded in a universal testing machine (Zwick/Roell Z10; Zwick, Ulm, Germany) to test the static fracture load. An indenter axially hit the occlusal surface of the specimen with a crosshead speed of 1 mm/min. The load which was necessary to initiate a crack (F_{initial}) and the load which was needed to completely fracture the specimen (F_{max}) were measured. The type of failure was specified under a stereomicroscope ($9\times$ magnification; Leica DFC300 FX; Wetzlar, Germany) and on photographs. The following scores were categorized: (1) score 0 = no visible fracture, (2) score 1 = cohesive fracture within the restoration, (3) score 2 = cohesive fracture of the restoration and of the cement layer, (4) score 3 = fracture of the restoration-cement-tooth complex.

2.8. Statistical analysis

The metric variables (F_{initial} , F_{max}) were described with mean, median, standard deviations, quartiles, minimum and maximum. They were compared using a non-parametric Kruskal-Wallis test (KW). The exact p-values were calculated for the pair-wise comparisons between the groups using the Wilcoxon-Mann-Whitney-Test (WMW), applying the Bonferroni correction for the multiple testing.

The categorical variables (failure scores) were summarized by counts and proportions of the categories and compared applying the Chi-squares test with exact determination of the p-value.

3. Results

3.1. Fatigue resistance

All specimens of all groups survived the thermo-mechanical aging without any technical complication. Therefore, all specimens were able to be further loaded until fracture in the static loading test.

3.2. Load-bearing capacity

The median F_{initial} values (and first Q1 and third Q3 quartiles) for the groups 3DP, CAM and HPR were 1'650 N (Q1:

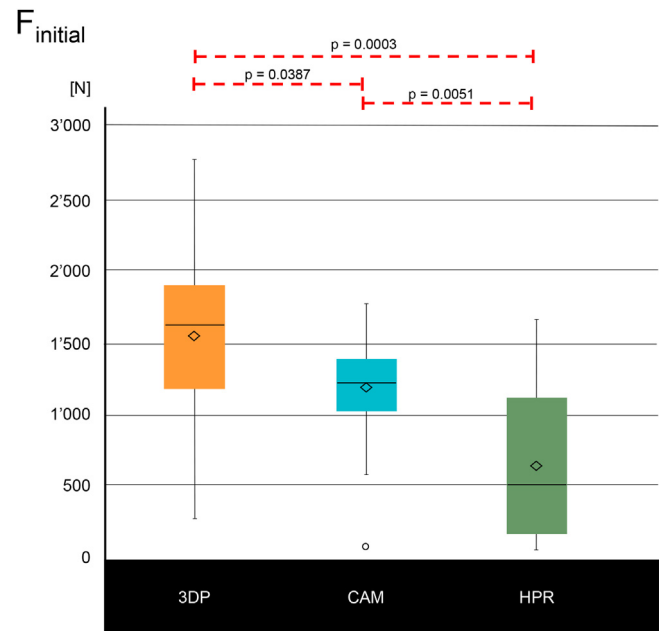


Fig. 4 – Box plots for F_{initial} values of the groups 3DP, CAM and HPR with significant differences marked with a dashed red bar and with the given exact p-values of the Wilcoxon-Mann-Whitney-Test.

1200, Q3: 1900), 1'250 N (Q1: 1'050, Q3: 1'400) and 500 N (Q1: 143, Q3: 1'100) (Table 2, Fig. 4). In group 3DP values ranged between 250 and 1'900 N. The minimum value in group CAM was 100 N, whereas 1'800 N was the highest reached F_{initial} value. The range in group HPR was between 40 and 1'700 N. All three groups showed statistically significant differences for F_{initial} (KW $p < 0.0001$) between each other. The exact p-values amounted $p = 0.0387$ (WMW) for the comparison 3DP – CAM, $p < 0.003$ for the comparison 3DP – HPR and $p = 0.0051$ for the comparison CAM – HPR.

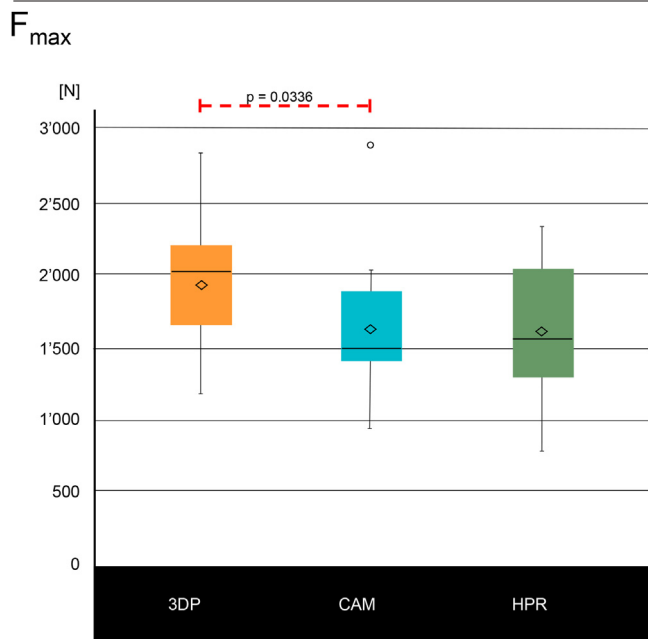
The median (and first Q1 and third Q3 quartiles) of the F_{max} values were: 2'025 N (Q1: 1'664, Q3: 2'184) for 3DP, 1'500 N (Q1: 1'423, Q3: 1'907) for CAM and 1'555 N (Q1: 1308.5, Q3: 2050) for HPR (Table 2, Fig. 5). The F_{max} values of group 3DP ranged between 1'189 and 2'808 N, whereas the minimal and maximal values of group CAM were 952 and 2'879 N respectively. In the group HPR the minima and maxima were 795 and 2'337 N. The Kruskal-Wallis test showed significant differences between the groups ($p = 0.0238$). The significances were found for the comparison 3DP-CAM (exact p-value WMW: $p = 0.0336$)

3.3. Failure types

The distribution of failure types was analyzed with a Chi-square test (Fig. 6). No group showed Score 0 fractures. Score 1 fractures were detected in 15% of the HPR specimens. 85% of the HPR specimens were attributed to Score 2 and 5% to Score 3 fractures. In the groups 3DP and CAM, half of the specimens showed Score 2 and half of the specimens Score 3 fractures. Significant differences were found between the three groups ($p = 0.0016$). Group HPR showed a higher incidence of score 1 fractures and a lower incidence of score 3 fractures than statistically expected.

Table 2 – F_{initial} and F_{max} values for the groups 3DP, CAM and HPR with means and standard deviation, median, 1. quartiles (Q1), 3. quartiles (Q3), minima (min) and maxima (max). Values in Newton.

Group	n	F_{initial}					F_{max}				
		Mean \pm SD	Q1	Median	Q3	Range min to max	Mean \pm SD	Q1	Median	Q3	Range min to max
3DP	20	1'583 \pm 542	1,200	1'650	1'900	250–2'800	1'928 \pm 396	1,665	2'026	2'184	1'189–2'808
CAM	20	1'215 \pm 407	1,050	1,250	1,400	100–1'800	1'635 \pm 410	1,423	1,500	1,907	952–2'879
HPR	20	662 \pm 568	143	500	1,100	40–1'700	1'614 \pm 422	1,309	1,555	2,050	795–2'337

**Fig. 5 – Box plots for F_{max} values of the groups 3DP, CAM and HPR with significant differences marked with a dashed red bar and with the given exact p-value of the Wilcoxon–Mann–Whitney-Test.**

4. Discussion

For the first time, the LCM technique was applied for the fabrication of 3D-printed zirconia restorations. The present investigation showed that 3D-printed zirconia ultra-thin occlusal veneers exhibited similar or higher load-bearing capacities as compared to heat-pressed lithium disilicate or CAD/CAM milled zirconia occlusal veneers.

All tested specimens survived aging procedures without any technical complication, indicating that 3D-printed zirconia, milled zirconia and heat-pressed lithium disilicate restorations in a thickness of 0.5 mm may withstand normal clinical conditions. The artificial aging included 1'200'000 dynamic loading cycles of 49 N in a frequency of 1.67 Hz with thermo-cycling between 5–55 °C and was reported to simulate 5 years of clinical service [21–23]. Chewing forces, however, are known to be higher than 49 N and may vary from 200 to 540 N [24]. In patients suffering from bruxism, values of up to 800 N were measured [24]. Considering the median F_{initial} values ranging from 500 N (HPR) to 1'250 N (CAM) and 1'650 N (3DP), it may be assumed that all the tested restorative materials would withstand regular clinical conditions.

In the present study, the measured F_{initial} and F_{max} values in each group were higher than the flexural strength values provided by the manufacturers of the tested restoration materials. Flexural strength of 3D-printed zirconia in group 3DP is reported to be 800 MPa, the zirconia in group CAM

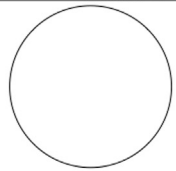


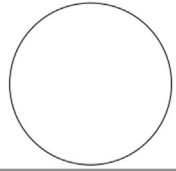





	score 1	score 2	score 3
3DP	 0%	 50%	 50%
CAM	 0%	 50%	 50%
HPR	 15%	 80%	 5%

Fig. 6 – Distribution of failure types for the groups 3DP, CAM and HPR. No visible fracture (score 0) was not seen in any of the groups. For the cohesive fracture within the restoration (score 1), cohesive fracture of the restoration and of the cement layer (score 2) and fracture of the restoration-cement- tooth complex (score 3) representative pictures and the distribution in % are depicted.

exhibits 700 MPa, whereas for heat-pressed lithium disilicate ceramic in group HPR 470 MPa are expected. In this study, however, the load-bearing capacity of the specimens was tested, which includes the entire tooth-cement-restoration complex and therefore resulted in much higher values. Apparently, the sequence of median F_{initial} -values with 1'650 N (3DP), 1'250 N (CAM) and 500 N (HPR) met the expectations derived from the mechanical properties provided by the manufacturers. F_{initial} represents the load which is needed to form a crack in the tested specimen. Thus, the crack formation started at the lowest loads in the lithium disilicate restorations, while the zirconia restorations showed a crack formation at higher states. This is in accordance with studies showing that zirconia has a better mechanical performance than lithium disilicate ceramic [8,14]. Despite the high median capability of 3D printed zirconia to withstand loads which lead to crack formation, the deviation of the recorded values was high. This might be attributed to the fabrication method of 3D printed restorations which involves a postprocessing by debinding the green part from the organic photopolymer matrix. Therefore, future developments should aim to investigate the influence of postprocessing on the consistency of the mechanical performance of 3D printed zirconia. In all groups, a complete fracture of the specimens (F_{max}) was observed at much higher values with medians of 2'026 N for 3DP, followed by 1'555 N for HPR and 1'500 N for CAM. The greatest increase was observed in the specimens with lithium disilicate ceramic occlusal veneers. It may be hypothesized that the strong adhesive bond between lithium disilicate and the abutment tooth is able to compensated the inferior mechanical property of the material compared to the zirconia restorations and positively influenced the load-bearing for lithium disilicate occlusal veneers thereby [25].

The specimens with 3D printed zirconia showed the same fracture patterns as the ones with milled zirconia. In both groups with zirconia, half of the fractures occurred within the restoration and the cement layer (score 2) and half of the fractures affected the entire restoration-cement-tooth complex (score 3). In contrast, for lithium disilicate 95% of all specimens showed fractures within the restorative material (score 1) or the restorative material and the cement layer (score 2). Score 1 and 2 fractures indicate that static loading forces are able to break the restoration and the adhesive bond but not the natural tooth itself. Score 3 fractures, however, involve a fracture of the entire restoration-cement-tooth complex and thus indicate that the mechanical resistance of the restorative material surpasses the mechanical strength of the tooth itself. With zirconia being a restorative material showing higher flexural strength than lithium disilicate, the distribution of fracture patterns seems reasonable.

In this study, a non-translucent zirconia was used for the production of the 3DP specimens. Regarding the optical properties, this type of zirconia may not be an ideal restoration material for occlusal veneers. The optical and mechanical properties of zirconia are related to the chemical composition (REF 31034947). Conventional zirconia with 3 mol% Y_2O_3 stabilized ZrO_2 showed excellent mechanical properties but are known to be opaque [26]. The translucency of zirconia was increased by a change in the percentages of Yttria and Alumina, the grain size, the use of different dopants

and stabilizers [27–29]. By adapting the chemical composition of zirconia intermediate physical properties were obtained ranging between conventional zirconia and lithium disilicate [28,30]. The comparison of two zirconia materials with differing chemical compositions may be seen as a limitation of the present study. The aim of the present investigation, however, was to present a proof of principle for the processing and mechanical performance of 3D printed occlusal zirconia veneers, as this method has not been approved by other studies yet.

For the minimally invasive reconstruction of the worn posterior dentition, high translucent milled zirconia or heat-pressed lithium disilicate are both materials that can be recommended clinically. Occlusal veneers made by 3D printing zirconia, showed promising results regarding their mechanical properties. Further efforts have to be made to increase the translucency of zirconia used for 3D-printing by the LCM technique.

5. Conclusions

Regarding their load-bearing capacity, CAD/CAM 3D-printed or subtractive CAD/CAM milled zirconia as well as heat-pressed lithium disilicate can be recommended to fabricate ultra-thin occlusal veneers to prosthetically compensate for occlusal tooth wear. Despite statistically significant differences between the restoration materials, all load-bearing capacities exceeded the clinically expected normal bite forces.

Acknowledgements

The authors express their thank to Falko Noack, Chistoph Giessmann, Albert Trottmann, Andrea Patrizi and Raphael Laue for their help in the fabrication procedures. The current study is part of and in parts identical with the master's thesis "Load-bearing capacity of ultra-thin occlusal veneers on molars, comparing 3D-printed zirconia, CAD/CAM-fabricated zirconia and heat-pressed lithium disilicate ceramic reconstructions: an in-vitro study" by the co-author Olivia Birrer, performed at the University of Zurich, Switzerland, under the supervision of Alexis Ioannidis and Christoph Hämmerle.

REFERENCES

- [1] Varma S, Preiskel A, Bartlett D. The management of tooth wear with crowns and indirect restorations. *Br Dent J* 2018;224:343–7.
- [2] Edelhoff D, Sorensen JA. Tooth structure removal associated with various preparation designs for posterior teeth. *Int J Periodontics Restorative Dent* 2002;22:241–9.
- [3] Muts EJ, van Pelt H, Edelhoff D, Krejci I, Cune M. Tooth wear: a systematic review of treatment options. *J Prosthet Dent* 2014;112:752–9.
- [4] Alkadi L, Ruse ND. Fracture toughness of two lithium disilicate dental glass ceramics. *J Prosthet Dent* 2016;116:591–6.
- [5] Guess PC, Selz CF, Steinhart YN, Stampf S, Strub JR. Prospective clinical split-mouth study of pressed and CAD/CAM all-ceramic partial-coverage restorations: 7-year results. *Int J Prosthodont* 2013;26:21–5.

- [6] Ioannidis A, Mühlemann S, Özcan M, Hüsler J, Hämmerle CH, Benic G. Ultra-thin occlusal veneers bonded to enamel and made of ceramic or hybrid materials exhibit load-bearing capacities not different from conventional restorations. *J Mech Behav Biomed Mater* 2019;433–40.
- [7] Chevalier J. What future for zirconia as a biomaterial? *Biomaterials* 2006;27:535–43.
- [8] Denry I, Kelly JR. State of the art of zirconia for dental applications. *Dent Mater* 2008;24:299–307.
- [9] Tinschert J, Natt G, Hassenpflug S, Spiekermann H. Status of current CAD/CAM technology in dental medicine. *Int J Comput Dent* 2004;7:25–45.
- [10] Schwentenwein M, Homa J. Additive manufacturing of dense alumina ceramics. *Int J Appl Ceram Technol* 2014;12:1–7.
- [11] Ebert J, Ozkol E, Zeichner A, Uibel K, Weiss O, Koops U, et al. Direct inkjet printing of dental prostheses made of zirconia. *J Dent Res* 2009;88:673–6.
- [12] Al-Akhali M, Chaar MS, Elsayed A, Samran A, Kern M. Fracture resistance of ceramic and polymer-based occlusal veneer restorations. *J Mech Behav Biomed Mater* 2017;74:245–50.
- [13] Guazzato M, Albakry M, Ringer SP, Swain MV. Strength, fracture toughness and microstructure of a selection of all-ceramic materials. Part I. Pressable and alumina glass-infiltrated ceramics. *Dent Mater* 2004;20:441–8.
- [14] Guazzato M, Albakry M, Ringer SP, Swain MV. Strength, fracture toughness and microstructure of a selection of all-ceramic materials. Part II. Zirconia-based dental ceramics. *Dent Mater* 2004;20:449–56.
- [15] Ma L, Guess PC, Zhang Y. Load-bearing properties of minimal-invasive monolithic lithium disilicate and zirconia occlusal onlays: finite element and theoretical analyses. *Dent Mater* 2013;29:742–51.
- [16] Maeder M, Pasic P, Ender A, Özcan M, Benic G, Ioannidis A. Load-bearing capacities of ultra-thin occlusal veneers bonded to dentin. *J Mech Behav Biomed Mater* 2019;95:165–71.
- [17] Körber K, Ludwig K. The maximum bite force as a critical factor for fixed partial dentures. *Dent Labor* 1983;31:55–60.
- [18] Schwentenwein M, Homa J. Additive manufacturing of dense alumina ceramics. *Int J Appl Ceram Technol* 2015;12:1–7.
- [19] Homa J, Schwentenwein M. A novel additive manufacturing technology for high-performance ceramics. *Ceram Eng Sci Proc* 2015:33–40.
- [20] Krejci I, Reich T, Lutz F, Albertoni M. An in vitro test procedure for evaluating dental restoration systems. 1. A computer-controlled mastication simulator. *Schweiz Monatsschr Zahnmed* 1990;100:953–60.
- [21] Bates JF, Stafford GD, Harrison A. Masticatory function — a review of the literature. 1. The form of the masticatory cycle. *J Oral Rehabil* 1975;2:281–301.
- [22] DeLong R, Douglas WH. An artificial oral environment for testing dental materials. *IEEE Trans Biomed Eng* 1991;38:339–45.
- [23] Steiner M, Mitsias ME, Ludwig K, Kern M. In vitro evaluation of a mechanical testing chewing simulator. *Dent Mater* 2009;25:494–9.
- [24] Bates JF, Stafford GD, Harrison A. Masticatory function — a review of the literature. III. Masticatory performance and efficiency. *J Oral Rehabil* 1976;3:57–67.
- [25] Lim MJ, Lee KW. Effect of adhesive luting on the fracture resistance of zirconia compared to that of composite resin and lithium disilicate glass ceramic. *Restor Dent Endod* 2017;42:1–8.
- [26] Kwon SJ, Lawson NC, McLaren EE, Nejat AH, Burgess JO. Comparison of the mechanical properties of translucent zirconia and lithium disilicate. *J Prosthet Dent* 2018;120:132–7.
- [27] Jiang L, Liao Y, Wan Q, Li W. Effects of sintering temperature and particle size on the translucency of zirconium dioxide dental ceramic. *J Mater Sci Mater Med* 2011;22:2429–35.
- [28] Carrabba M, Keeling AJ, Aziz A, Vichi A, Fabian Fonzar R, Wood D, et al. Translucent zirconia in the ceramic scenario for monolithic restorations: a flexural strength and translucency comparison test. *J Dent* 2017;60:70–6.
- [29] Sulaiman TA, Abdulmajeed AA, Donovan TE, Ritter AV, Vallittu PK, Narhi TO, et al. Optical properties and light irradiance of monolithic zirconia at variable thicknesses. *Dent Mater* 2015;31:1180–7.
- [30] Zhang F, Reveron H, Spies BC, Van Meerbeek B, Chevalier J. Trade-off between fracture resistance and translucency of zirconia and lithium-disilicate glass ceramics for monolithic restorations. *Acta Biomater* 2019;91:24–34.